

EXHIBIT 25

ADHESION AND AERODYNAMIC RESUSPENSION OF FIBROUS PARTICLES

By Nurtan A. Esmen¹

ABSTRACT: Under a simplifying assumption of uncharged particles, the adhesion theory was used in conjunction with the boundary layer theory to derive an expression for the lower limit of velocity for the resuspension of fibrous particles from flat surfaces. The theory, albeit approximate, suggests that mineral fibers with diameters less than 9 μm diameter will not be resuspended by bulk air velocities less than 10 m/s. Since electrostatic forces, fiber orientation or high humidity will require a higher aerodynamic force to lift the fibers off a surface, this theoretical limit is conservative for environmental exposure considerations. The theoretical calculations were experimentally confirmed by observing the behavior of settled single fibers in turbulent air flow. The results of the theoretical analysis and the subsequent experimental confirmation suggests that the concerns about the aerodynamic resuspension of mineral fibers within a biologically significant size range are overstated.

INTRODUCTION

The concern for the health effects of inhalation of fibrous aerosols with special emphasis on asbestos has led to a number of claims in court proceedings and other forums suggesting extensive resuspension of deposited fibrous particles due to the normal air currents found in a work place or general environment [e.g., Environmental (1989); U.S. Court (1990)]. The fiber diameter and length requirements related to the disease causing potential of fibrous aerosols suggest that the concerns with respect to the inhalation of fibers must be restricted to those, biologically significant, fibers that can penetrate beyond the human nasopharyngeal compartment. The theoretical and experimental evidence available on isometric particles suggest that the general claims of the resuspension of biologically significant fibers by normally encountered work place or environmental air flow may be overstated (Corn 1966; Fletcher 1976a; 1976b; Zimon 1980; Hinds 1982). Therefore, the concerns expressed with respect to fibrous aerosol resuspension, contrary to the available information, justify a specific investigation of fibrous particle resuspension; at least, for a better understanding of the general limits of resuspension of fibrous aerosols.

The adhesion of a particle to a surface and the removal of the particle from that surface by an external force can only be expressed with an associated probability of adhesion or removal. In the case of randomly oriented anisometric particles, such as fibers, the orientation of the external removal force with respect to the particle axes will superimpose another probability distribution associated with orientation onto the probability distribution associated with adhesion. In addition, due to the surface characteristics such as roughness, important theoretical complications exist in both the air flow and particle adhesion. Therefore, the complete theoretical analysis of the aerodynamic resuspension of particles from flat surfaces is complicated and hitherto intractable. However, through defining resuspension of a particle by the limiting value of the external force below which the probability of removal is negligible, the theoretical analysis can be made tractable. Clearly, under this assumption only the forces normal to the major axis of an anisotropic particle need to be considered.

The limiting values for the fibrous particle size and the environmental air flow are necessary in order to relate the the-

oretical analysis to environmental engineering problems. In general, the inhalation and respiratory system deposition of fibrous aerosols are governed by the aerodynamic diameter of the fibers, whereas the adhesion properties of a fiber is related to its geometric diameter. Without considering the regulatory limitations on the fiber, an upper limit for biologically significant fiber diameter may be calculated from the respiratory deposition characteristics of fibers. The upper size limit for thoracic aerosols for nearly isometric particles is $21 \pm 2 \mu\text{m}$ aerodynamic equivalent diameter (Vincent 1989), thus for a minimum aspect ratio of 5 and for a mineral fiber density of $2500\text{--}2900 \text{ kg/m}^3$, the maximum biologically significant fiber diameter may be calculated by (Burke and Esmen 1978)

$$D_f = \frac{D_g}{\sqrt{\rho_p(0.7 + 0.91 \ln \beta)/1000}}$$

$$= \frac{19 \times 10^{-6}}{\sqrt{2.9(0.7 + 0.91 \ln 5)}} = 8.6 \times 10^{-6} \quad (1)$$

Based on analyses of the available empirical data, the upper limit for fiber diameter in thoracic deposition was shown to be significantly smaller than 10 μm (Kahn and Esmen 1988; Lippmann 1988; Esmen and Erdal 1990). Therefore, a 43 μm long, 8.6 μm diameter mineral fiber may be reasonably but conservatively selected as the upper size limit for biologically significant fibrous aerosols.

THEORETICAL CONSIDERATIONS

When a fiber (or any shape particle) settles on a surface, it is held there by a number of forces that operate on the microscopic level. These forces are molecular interaction mainly represented by London-van der Waals forces, electrostatic forces and the surface tension of the condensed layer of fluid between a particle and a surface. If the fiber is not charged or the surface is a properly grounded conducting surface, then the contribution of electrostatic attraction to adhesion is precluded. The electrostatic effects are important for the generalized understanding of adhesion. However, between and within most particle adhesion studies a several fold variability is common and any empirical data used for the evaluation of the semiempirical constants would probably contain the electrostatic effects "on the average" unless a considerable care is taken to nullify such effects. Consequently, the complications introduced by the inclusion of the electrostatic effects is unnecessary for an investigation of the limiting behavior in particle resuspension.

The integrated form of the adhesion equation for a sphere resting on a surface is known as the Bradley-Hamaker equation. Dahneke (1972) extended the adhesion equation to include the mechanical properties of the surface and the particle as well as repulsive forces. In that formulation, the influence

¹Prof. of Occupational and Envir. Health, Univ. of Oklahoma—Health Sciences Ctr., CHB 413, P.O. Box 26901, 801 NE 13th Street, Oklahoma City, OK 73190.

Note. Associate Editor: Lynn M. Hildemann. Discussion open until October 1, 1996. To extend the closing date one month, a written request must be filed with the ASCE Manager of Journals. The manuscript for this paper was submitted for review and possible publication on January 3, 1995. This paper is part of the *Journal of Environmental Engineering*, Vol. 122, No. 5, May, 1996. ©ASCE, ISSN 0733-9372/96/0005-0379-0383/\$4.00 + \$.50 per page. Paper No. 9863.

of interaction between two surfaces are related to the deformation (elasticity properties) of the two surfaces in contact. The two elastic constants needed in the expression of deformation are Young's modulus of elasticity and Poisson's ratio. The increase in the adhesive force due to deformation added to the Bradley-Hamaker adhesive force may be used to calculate the maximum adhesive force

$$F_{\max} = \frac{AD}{12z_0^2} \left[1 + \frac{A^2 K_p^2 D}{108z_0^7} \right]$$

$$\text{and } K_p = \frac{Y_1(1 - \nu_2^2) + Y_2(1 - \nu_1^2)}{Y_1 Y_2} \quad (2)$$

For hard materials such as mineral fibers on hard surfaces such as glass or steel the expression in the brackets may be shown to be only a few percent larger than 1, thus the expression for the adhesive force may be simplified to a linear expression; that is the particle diameter multiplied by a constant

$$F_{\text{adh}} = \frac{AD}{12z_0^2} = C_H D \quad (3)$$

The capillary condensation and adsorption of water vapor are expected to occur at normally occurring relative humidity around the particles resting on a smooth surface. The adhesive effect of the condensed fluid is additive with respect to the adhesion forces and may be accounted for by a simple correction to the Bradley-Hamaker equation (Hinds 1982)

$$F_{\text{adh}} = C_H D(1 + 0.009 \cdot H) \quad (4)$$

Since the earliest studies of reentrainment of particles, it has been reported that the particles first slide or roll before dislodgment (Corn 1966). Thus the resuspension of particles is related to an adhesive drag rather than the total adhesive force which is related to the actions that tend to pull a particle off a surface. The recent theories of molecular basis of adhesion and friction suggest a lack of static threshold force to initiate motion (Cieplak et al. 1994) and the rate of separation is a time and force dependent entity (Kendall 1994). The adhesion constant C_H of (4) represents a maximum (static adhesion) and it is considerably larger than the dynamic adhesive friction operative in the dislodgment of particles. The adhesion data which reports dislodgment forces parallel to the surface suggests that the dynamic adhesion coefficient is about 1% of the static adhesion coefficient (Stein and Corn 1965; 1966).

The effect of the anisotropy of the fibers on the adhesive forces must also be accounted for. Although a direct theoretical expression of the effect of particle shape is not available, a heuristically defined shape factor that can be used to modify the adhesive forces defined for isotropic particles may be developed by analogy to an available theoretical analysis. The analysis of molecular forces between randomly oriented cylinders by Vold (1954) suggests that the adhesion between cylinders is always larger than adhesion between spherical particles of equal volume. An estimate of the increase in the fiber—surface adhesion from the theoretical results is not tractable. However, by direct analogy, it may be suggested that the increase in the adhesive force between a surface and a fiber is related to the ratio of circumferences of contact. With the diameter of an equivalent sphere defined by $(3\beta/2)^{1/3}D$, an adhesion shape factor may be shown to be

$$K_c = \frac{2(\beta + 1)}{\pi(3\beta/2)^{1/3}} = \frac{(\beta + 1)}{1.7981\beta^{1/3}} \quad (5)$$

Thus, using the shape factor suggested in (4) and empirically observed reduction in value between a static and a dynamic adhesion coefficient, (4) may be generalized to describe the dynamic adhesive force for fibrous or isotropic particles

$$F_{\text{adh}} = \frac{(\beta + 1)}{1.7981\beta^{1/3}} C_0 D(1 + 0.009 \cdot H); \quad C_0 \sim 0.01 C_H \quad (6)$$

Without a mechanical force to eject a fiber into an air stream, a fiber can only be resuspended if it is mobilized by the turbulent air flow of an environment. Thus, in the investigation of particle resuspension, the first consideration is the structure of the turbulent flow field near a surface in the scale of the particle size. In the characterization of turbulent flow near solid surfaces, the orthogonal distance to the surface is usually represented by a dimensionless distance, that is by a number similar to Reynolds' number. In the constant shear stress region of the flow (Boundary Layer) the ratio of the shear stress to fluid density has the dimensions of speed squared and they are used to define an entity called friction velocity. The friction velocity, kinematic viscosity of the fluid and the distance to the wall are the defining parameter of the dimensionless distance. The boundary layer theory for turbulent flow over a solid surface suggests that for the values of the dimensionless distance $z^+ < 5$, the flow is viscous and the velocity component parallel to the surface is [cf. Brodkey (1967) or Schlichting (1960)]

$$U(z) = U_* z^+ \text{ for all } z^+ = \frac{z U_*}{\nu} \cong 0.0395 U_* R_s^{-1/8} \left(\frac{z}{\nu} \right) < 5 \quad (7)$$

The evaluation of (7) for all $R_s > 3000$, and $U_* < 34$ m/s, shows that all particles with $D < 30 \mu\text{m}$ resting on a solid surface would be wholly submerged within the viscous sublayer.

Phillips (1980) proposed a force balance model for the resuspension of small particles by turbulent flow. In this model, the entrainment takes place if the force due to either the aerodynamic lift or the penetrative turbulent updraft exceeds the sum of difference of adhesive and buoyant forces. The force due to the updrafts of anisotropic penetrative eddies was shown to be the dominant resuspension mechanism for particles that are wholly in the viscous sublayer. This force is proportional to the third power of the friction velocity based particle Reynolds' number (Cleaver and Yates 1973). With $K_v = 3/2$ or 1 for a cylinder or for a sphere respectively, the force balance proposed by Phillips (1980) may be generalized to include cylindrical particles

$$C_2 \rho_f \nu^2 \left(\frac{U_* D}{\nu} \right)^3 = \frac{(\beta + 1)}{1.7981\beta^{1/3}} C_0 D(1 + 0.009 \cdot H)$$

$$+ \frac{\pi}{6} K_v \beta D^3 \rho_f g; \quad U_* = k_f U_w \quad (8)$$

Phillips (1980) reported that $C_2 = 21$ for air and $C_0 = 1.43 \times 10^{-5}$ N/m as determined from the dust resuspension data of Fletcher (1976a). This particular value of C_0 represents the entrainment of particles from a "dust pile" with an unreported relative humidity. This value is considerably less than $C_0 = 1 \times 10^{-3}$ N/m for monolayer particles (Corn and Stein 1965; 1966). Though the apparent entrainment from a multilayer dust stratum is expected to be lower than that of a monolayer stratum, nearly two orders of magnitude difference would not be expected.

Some earlier models unsuccessfully attributed the lifting of the particle to the drag force (Corn 1966) by a dichotomous mechanism such that when the drag exceeds adhesion, the particle detaches from the surface. Phillips (1980) showed that the direct aerodynamic lift is applicable only to the particles that project into nearly isotropic turbulent flow beyond the viscous sublayer. In contrast to a dichotomous model, the drag force may be considered to operate on adhesion linearly to reduce friction. Thus, it may be conceptualized that the sudden penetrative turbulent uplift is responsible for resuspension of

particles in conjunction with the linear reduction of friction due to drag. With the velocity distribution is as determined by (7), the stagnation pressure averaged over the height of a particle is

$$P = \frac{1}{D} \int_{z=0}^{z=D} \frac{1}{2} \rho_f U^2(z) dz = \frac{1}{6} \rho_f \frac{D^2 U_*^4}{v^2} \quad (9)$$

Consequently

$$F_D = C_D P \beta D^2 K_A = \frac{C_D}{6} \rho_f v^2 R_p^4 \beta K_A \quad (10)$$

Within the viscous sublayer, for particles resting on a surface, neither a precise theoretical nor an experimental quantification of the effect of the wall on drag has been reported. It may be, intuitively, suggested that the use of (9) and (10) would be expected to account for the wall effect. Thus the friction coefficient as a function of the drag force is

$$C_1 = C_0 \left[1 - \frac{F_D}{F_F} \right] \text{ for } F_D < F_F \quad (11)$$

For cylinders the drag coefficient may be estimated from the data and formula reported by Jones-Knudsen (1961)

$$C_D = \frac{9\pi}{R_p S} \left[1 - \left(s^2 - \frac{S}{2} + \frac{5}{16} \right) \frac{R_p^2}{32S} \right] \cdot \left[1 - \frac{\pi}{2} \exp(-0.6\beta^{1/2}) \right]; \quad S = 2.0022 - \ln R_p \quad (12)$$

Since friction velocity for the boundary layer for a flat plate is approximately 6% of the characteristic velocity of the system, then for $D < 20 \mu\text{m}$ and $U_\infty < 30 \text{ m/s}$, (12) can be simplified

$$C_D = \frac{9\pi}{R_p (2.0022 - \ln R_p)} \left[1 - \frac{\pi}{2} \exp(-0.6\beta^{1/2}) \right] = \frac{f_c(R_p, \beta)}{R_p} \quad (13)$$

and the drag coefficient formula for a sphere is (Hinds 1982)

$$C_D = \frac{24}{R_p} \left[1 + \frac{R_p^{2/3}}{6\beta} \right] = \frac{f_s(R_p, \beta)}{R_p}, \quad \beta = 1 \quad (14)$$

Thus the general equation for the aerodynamic resuspension of particles is

$$v^2 \rho_f R_p^3 \left[C_2 + \frac{\beta K_A}{6} f(R, \beta) \right] = \frac{(\beta + 1)}{1.7981\beta^{1/3}} C_0 (1 + 0.009H) D + \frac{\pi}{6} K_v \rho_p \beta D^3 g \quad (15)$$

The reevaluation of Fletcher (1976a) and Corn and Stein (1965; 1966) data by (15) suggest that C_0 are approximately 8×10^{-5} and 9×10^{-4} for multi- and monolayer dusts, respectively. The theoretical consideration of the difference between multi and monolayered dusts is beyond the scope of this work. However, an approximately 10 fold difference is reasonable and can be explained in terms of the flow penetration into the substrate and the entrainment of agglomerates for multilayered dusts. By assuming 0.06 as the friction factor for the flow and $2,900 \text{ kg/m}^3$ for mineral fiber density, the limiting ambient air speed for the resuspension of mineral fiber aerosols may be calculated by (15). Fig. 1 shows the calculated minimum ambient air speed necessary for the resuspension of fibers with aspect ratio of 5 as a function of fiber diameter and two relative humidity levels. Thus, for an $8.6 \mu\text{m}$ by $43 \mu\text{m}$ fiber resting on a surface at 50% relative humidity, the mini-

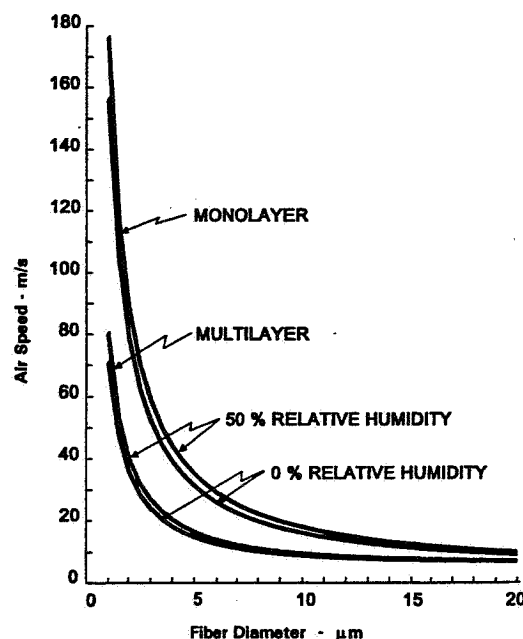


FIG. 1. Calculated Minimum Air Speed Necessary for Resuspension of Fibers as Function of Fiber Diameter ($\beta = 5$)

mum required air speeds for resuspension from multi- and monolayers are 10.2 and 20.7 m/s respectively.

EXPERIMENTAL VERIFICATION OF FIBER REDISPERSION LIMIT

The experimental verification of the theoretical results was based on the continuous observation of single fibers until the induction of their motion by the influence of a steadily increasing air speed. The experimental fibers were produced by chopping spun strands of either $10 \mu\text{m}$ (0.00040 inch—type H) or $15 \mu\text{m}$ (0.00060 inch—type M) nominal diameter, continuously formed glass fiber threads in an ordinary electric coffee grinder. A bundle of approximately 5 cm long spun fiber strands were fluffed by hand and were ground for a few minutes. The grinder was emptied on a large flat mirror using a soft rubber spatula. Visibly long fibers and large clumps were removed with a pair of tweezers. After spreading the fibers over the mirror by shaking and brushing, the mirror was held at about 45 degrees up and tapped gently on edge several times to eliminate long fibers and large agglomerates. After this elimination process, the mirror was held vertically over a smooth aluminum foil and forcefully rapped on edge several times and/or gently brushed. These were sufficient to shake loose significant amount of fibers onto the foil. After discarding the shards and fibers that remained on the mirror, the grinding and selection process was repeated until sufficient amount of fibers for experimentation were obtained. An optical microscopic analysis showed that the medians of the diameter distribution were $10.6 \mu\text{m}$ and $16.1 \mu\text{m}$ with geometric standard deviations of 1.09 and 1.05 for the thinner and the thicker fibers respectively. In all transfer operations, the use of a mirror in conjunction with a beam of light is an important facilitator and a handy visual aid. Also, the use with frequent replacement of the highest quality soft sable artist's paint brushes with a flat edge is essential.

The fibers for each experiment were placed on the glass surface by blocking a standard glass microscope slide ($7.5 \text{ cm} \times 2.5 \text{ cm}$) by a thin aluminum shield with a sharp edged $3 \text{ mm} \times 6 \text{ mm}$ opening, parallel to and 1 cm away from one of the short edges. As small amount of experimental fibers as practicably transferable were put onto a small mirror and after the mirror edge was carefully placed vertically at the edge of

the opening, some of the fibrous dust was brushed down and the shield was removed. This procedure provided a sparse dust cover with at least one fiber within approximately 1 degree of the desired orientation; that is major axis orthogonal to the air velocity.

The 0.1 m × 0.2 m oblong cross section wind tunnel, shown schematically in Fig. 2, was designed to operate with airflow rates from 0.05 to 0.353 m³/s. At these flow rates, the flow in the wind tunnel is fully turbulent and velocity measurements by Pitot static traverse of the duct above the experimental section confirmed a fully developed turbulent velocity profile. The measured maximum velocity point was assumed to correspond to the virtual vertical center of the system and the velocity measurements at that point were used in all calculations and comparisons.

The experimental slide was placed flush with the bottom surface of the wind tunnel. Although the variation in the glass slide thickness is not large, a preselection of the slides vis-à-vis their thickness and their fit into the holder is important to minimize the disturbance of the flow upstream of the fibers. A fiber aligned within 1 degree of the perpendicular to the air flow was found by moving the microscope and its length was measured. The inverted microscope used had a 5X objective and 5X ocular equipped with an ordinary Whipple disc calibrated against a stage micrometer. A total fiber length of 400 μm could be measured directly in steps of 8 μm and estimated in steps of 4 μm. The initial velocity setting for each experiment was about 1/2 of the expected resuspension velocity and after about 30 seconds of stabilization, the air speed was slowly increased by closing the control gate with a servomotor driven screw. The rate of velocity pressure increase was about 65 mm of water/hr and it was nearly constant in the experimental range (5–23 m/s). The fiber was observed until it moved and the velocity pressure was noted at the moment of its motion. In all cases, the observed fiber stood still until it suddenly disappeared from the view. This observation, at least qualitatively confirms the penetrative turbulence model for particle entrainment into a fluid stream.

ANALYSIS OF RESULTS

There were 52 experiments with 10 μm fibers with fiber lengths ranging from 36 to 400 μm and 41 experiments with 16 μm fibers with fiber lengths ranging from 52 to 396 μm. In these experiments the air temperature was 17 ± 2°C and the Relative Humidity was 42 ± 5 percent. The comparison of the calculated and the measured resuspension air speeds are shown in Fig. 3. Even though the calculated values are, on the average, lower than the measured ones, the comparison shown suggests that there is a good agreement between the theoretical calculations and the experimental results. Possible differences in the surface characteristics of each type of fiber or the assumed friction coefficient for the theoretical calculations may be responsible for these differences. In fact, the variability of the calculated friction coefficients are even greater. Using the measured air speeds, the calculated average friction coefficients are 1.07×10^{-4} N/m and 1.35×10^{-4} N/m with standard deviations 4.52×10^{-5} N/m and 5.31×10^{-5} N/m for 10 and 16 μm fibers respectively. These two values differ statistically significantly at $\alpha = 0.01$ by both *t* and Welch tests. Although a number of explanations for this difference are possible, the scope of the experiments do not allow for further speculation.

The method used in this study of adhesion of fibers offer interesting possibilities for fundamental experiments for a better understanding of adhesion of particles and the experimental results, although confirm the essential parts of the theoretical approach in the resuspension of settled particles, expose a large number of both experimental and theoretical questions

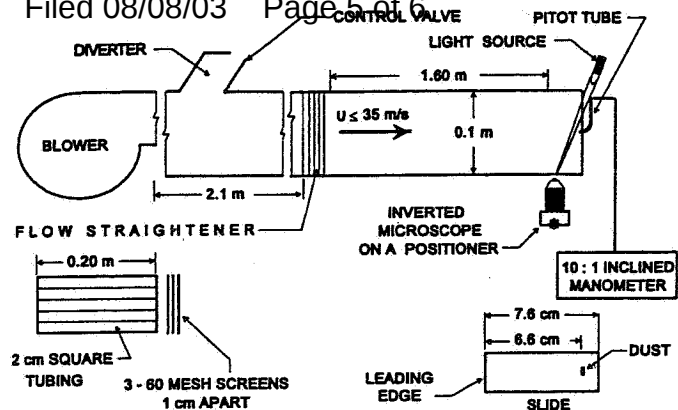


FIG. 2. Schematic Representation of 0.1 m × 0.2 m Oblong Cross Section Wind Tunnel and Experimental Apparatus

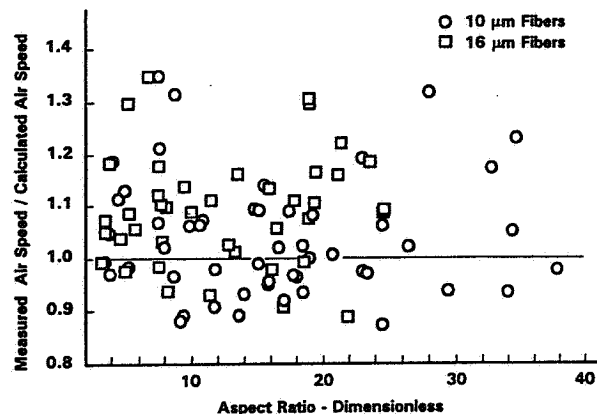


FIG. 3. Ratio of Measured Air Speed to Calculated Air Speed Necessary for Resuspension as Function of Fiber Aspect Ratio

that could be fascinating to study. However, both the potential benefits for further research and the further unanswered questions in particle adhesion are ancillary to the motivating factor for the research. Fortunately, vis à vis the original intent, the answer is clear. With the verification of about 10 m/s (36 km/h) as a theoretically calculated minimum air speed for the resuspension of biologically significant fibers under optimum conditions, i.e. fibers orthogonal to the air flow, significant or even minimal resuspension due to the normal air currents found in a work place or general environment is not to be expected.

The reason for the claims suggesting extensive resuspension of deposited fibrous particles due to the normal air currents must lie elsewhere. Agglomerated, spider web like loose structures of dust or fibers, sometimes referred to as "dust bunnies" in vernacular, sway, move about, break, and possibly travel some short distances. Unqualified observation of this behavior can suggest the possibility of fiber resuspension. By assembling structures similar to the loose agglomerates using the clumps and very long fibers rejected for experiment, the motion of such structures were observed. These structures moved at estimated air speeds as low 2 m/s. When the bottom of the structures were held in place by placing them in a pool of oil, the top part of some of the structures broke away at estimated air speed as low as 4 m/s; but the recovered fluffs did not show evidence of extensive fiber loss. Although the quantification of this action was not possible, the likelihood of extensive dispersion of fibers from such structures is unlikely unless they are buffeted about by large air velocities.

The theoretical and experimental conclusions are in concordance with the low observed environmental concentrations of fibers even in the locales with significant levels of environ-

mentally mediated mineral fiber exposure induced lung disease. As the origin for the environmentally observed levels of fibrous aerosols, mechanical dispersion mechanisms would be a more logical choice. Therefore, in the absence of idiosyncratic work such as digging, gardening, farming, house cleaning, playing in the dust etc. where a mechanical augmentation of air flow is responsible for the resuspension, the settled or surface adhered fibrous dusts would not be expected to present a health hazard. In general, the study of the fundamental processes of mechanical augmentation of particle resuspension is difficult both theoretically and experimentally. However, the results of this study suggest that such an investigation is essential for a rational understanding of the environmental implications of settled matter.

APPENDIX I. REFERENCES

- Brodkey, R. S. (1967). *The phenomena of fluid motions*. Addison Wesley, Reading, Mass., 244–256.
- Burke, W. A., and Esmen, N. A. (1978). "The inertial behavior of fibers." *Amer. Ind. Hyg. Assoc. J.*, 39(5), 400–405.
- Cieplak, M., Smith, E. D., and Robbins, M. O. (1994). "Molecular origins of friction: the force on adsorbed layers." *Science*, 265(5176), 1209–1214.
- Cleaver, J. W., and Yates, B. (1973). "Mechanism of detachment of colloidal particles from a flat substrate in a turbulent flow." *J. Colloid Interface Sci.*, 44(3), 464–474.
- Corn, M. (1966). "Adhesion of particles." *Aerosol science*, C. N. Davies, ed., Academic Press, New York, N.Y., 359–392.
- Corn, M., and Stein, F. (1965). "Re-entrainment of particles from a plane surface." *Am. Ind. Hyg. Assoc. J.*, 26(4), 325–336.
- Corn, M., and Stein, F. (1966). "Adhesion of atmospheric dustfall particles to a glass slide." *Nature*, 211(5044), 60–61.
- Dahneke, B. (1972). "The influence of flattening on the adhesion of particles." *J. Colloid and Interface Sci.*, 40(1), 1–13.
- Environmental Protection Agency (EPA). (1989). "40 CFR part 763 asbestos; manufacture, importation, processing, and distribution in commerce prohibitions—final rule." *Federal register*, 54(132), 29460–29495.
- Esmen, N. A., and Erdal, S. (1990). "Human occupational and nonoccupational exposure to fibers." *Envir. Health Perspectives*, 88, 261–268.
- Fletcher, B. (1976a). "The erosion of dust by an air flow." *J. Phys. D: Appl. Phys.*, 9, 913–924.
- Fletcher, B. (1976b). "The incipient motion of granular materials." *J. Phys. D: Appl. Phys.*, 9, 2471–2478.
- Hinds, W. C. (1982). *Aerosol technology*. John Wiley & Sons, Inc., New York, N.Y., 130.
- Jones, A. M., and Knudsen, J. G. (1961). "Drag coefficients at low Reynolds' numbers for flow past immersed bodies." *AIChE J.*, 7(3), 20–25.
- Kahn, R. A., and Esmen, N. A. (1988). "The deposition of fibers and spheres at the carina in excised lungs." *Proc., VIIth Int. Pneumococcosis Conf. DHHS (NIOSH) Publ. No. 90-108*, 1, 571–575.
- Kendall, K. (1994). "Adhesion: molecules and mechanics." *Science*, 263(5154), 1720–1725.

- Lippmann, M. (1988). "Asbestos exposure indices." *Envir. Res.*, 46(1), 86–106.
- Phillips, M. (1980). "A force balance model for particle entrainment into a fluid stream." *J. Phys. D: Appl. Phys.*, 13, 221–233.
- Schlichting, H. (1960). *Boundary layer theory*, 4th Ed., McGraw Hill, New York, N.Y.
- U.S. Court of Appeals for the Third Circuit. (1990). "Robertson et al. v. Allied Signal et al. and Drauschak et al. v. Allied Signal et al. appeals 89–2123 and 89–2124, opinion by Circuit Judge Massmann." *U.S. Courts*. G.M.C. Printing, Philadelphia, Pa.
- Vincent, J. H. (1989). *Aerosol sampling*. John Wiley and Sons, Inc. Chichester, U.K. 329.
- Vold, M. J. (1954). "Van der Waals' attraction between anisometric particles." *J. Colloid Sci.*, 9(4), 451–459.
- Zimon, A. D. (1980). *Adhesion of dust and powder*, 2nd Ed., Plenum, New York, N.Y.

APPENDIX II. NOTATION

The following symbols are used in this paper:

- A = Bradley-Hamaker Constant $O(10^{-19} \text{ J})$ (J);
- C_0 = friction coefficient (N/m);
- C_1 = dynamic friction coefficient (N/m);
- C_D = drag coefficient (N/m);
- C_H = adhesion coefficient (N/m);
- D = particle diameter (m);
- D_f = fiber diameter (m);
- D_e = aerodynamic equivalent diameter (m);
- F_{adh} = static adhesive force (N);
- F_F = dynamic adhesive force (N);
- F_D = drag force (N);
- F_{Max} = maximum adhesive force (N);
- $f(S, R_P)$ = drag coefficient function (\emptyset);
- g = gravitational constant (m/s^2);
- H = percent relative humidity (\emptyset);
- K_A = area factor (cylinder = 1, sphere = $\pi/4$) (\emptyset);
- K_C = adhesion shape factor (\emptyset);
- K_f = friction factor (\emptyset);
- K_P = plastic deformation coefficient (Pa^{-1});
- K_V = volume factor (cylinder = $3/2$, sphere = 1) (\emptyset);
- P = averaged stagnation pressure (Pa);
- R_P = particle Reynolds' number with U_* (\emptyset);
- R_S = system Reynolds' number (\emptyset);
- $U(z)$ = velocity component parallel to the surface (m/s);
- U_* = friction velocity (m/s);
- U_∞ = bulk velocity (m/s);
- v_i = Poisson's ratio (\emptyset);
- Y_i = Young's modulus of elasticity (Pa);
- z = distance normal to the surface (m);
- z^+ = dimensionless distance (\emptyset);
- z_0 = minimum approach distance between two surfaces (m);
- β = aspect ratio (length/diameter) (\emptyset);
- ρ_F = fluid density (kg/m^3);
- ρ_P = particle density (kg/m^3); and
- ν = kinematic viscosity (m^2/s).